

SUNSPOT TRANSITION REGION OSCILLATIONS IN NOAA 8156

N. Brynildsen, T. Leifsen, O. Kjeldseth-Moe, P. Maltby
*Institute of Theoretical Astrophysics, University of Oslo, P.O. Box 1029 Blindern,
0315 Oslo, Norway*

and

K. Wilhelm
Max-Planck-Institut für Aeronomie, D-37191 Katlenburg-Lindau, Germany

ABSTRACT

Based on observations obtained with the *Solar and Heliospheric Observatory - SOHO* joint observing program for velocity fields in sunspot regions, we have detected 3 min transition region umbral oscillations in NOAA 8156. Simultaneous recordings of O v $\lambda 629$ and N v $\lambda 1238$, $\lambda 1242$ with the SUMER instrument give the spatial distribution of power in the 3 min oscillations, both in intensity and line-of-sight velocity. Comparing loci with the same phase we find that the entire umbral transition region oscillates. The observed maxima in peak line intensity are nearly in phase with the maxima in velocity directed towards the observer. We discuss the suggestion that the waves are upward propagating acoustic waves.

Subject headings: Sun: magnetic fields — Sun: oscillations — Sun: transition region — Sun: UV radiation — sunspots

To appear in: *Astrophysical Journal Letters*

1. Introduction

The study of oscillations in the atmosphere of sunspots dates back to the detection of umbral flashes in the K line (Beckers & Tallant 1969), followed by the detection in H_{α} of penumbral waves (Zirin & Stein 1972, Giovanelli 1972) and umbral oscillations (Giovanelli 1972). The nature and mode identification of the 3 min oscillations in the umbral chromosphere have been debated. Based on linear theory two cavities have been discussed, i.e. a cavity for fast modes in the low photosphere and sub-photosphere and a cavity for resonant slow modes in the umbral chromosphere as well as a unified model with contributions from both cavities (e.g. Thomas & Weiss 1992). However, the 3 minute umbral oscillations in the chromosphere show a non-linear character, suggesting the presence of upward propagating shock waves (Lites 1992, Bard & Carlsson 1997). Knowledge of the oscillations in the transition region originates from the study of eight sunspots in the C IV $\lambda 1548$ line by Gurman et al. (1982), see also Henze et al. (1984). Interestingly, the observed waves with periods of 129 - 173 s, show no signs of shocks and appear to be upward propagating acoustic waves. Recently, Rendtel et al. (1998) reported transition region intensity oscillations in the 2 min range in sunspot NOAA 7986.

We focus on transition region sunspot oscillations in NOAA 8156, observed simultaneously in O v $\lambda 629$ and N v $\lambda 1238$, $\lambda 1242$. The observations were obtained on 1998 February 18 between 16:00 UT and 21:07 UT with the Solar Ultraviolet Measurements of Emitted Radiation (SUMER; Wilhelm et al., 1995) instrument as part of a joint observing program on the *Solar and Heliospheric Observatory (SOHO)*.

2. OBSERVATIONS

The pointing of the SUMER slit is kept constant to $525''$ W and $332''$ S off the solar disk center, i.e. at a heliocentric distance of 40° . The solar rotation moves the image of the sunspot, with umbral size $15''$ and penumbral size $50''$, over the narrow slit, $0.3'' \times 120''$. From each spectrum $90'' \times 2.2 \text{ \AA}$ spectral windows, centered on O v $\lambda 629$ and N v $\lambda 1238$, $\lambda 1242$, are recorded with detector B. With an exposure time of 15 s it takes 20 min to observe 80 consecutive spectra, called one raster, while the solar rotation moves the image $2.2''$. Figure 1 (bottom) shows the positions of the 12 rasters and the location of the sunspot, between $300''$ and $350''$ S off disk center. Between

each raster, exposures with the rear slit camera give the slit position in relation to the sunspot and 100 s exposures of $90'' \times 40 \text{ \AA}$ spectra give the wavelength scale, from the wavelength positions of chromospheric lines. The data reductions include corrections for the fixed pattern noise, defects of the detector and corrections for the geometrical distortions, see Wilhelm et al. (1995). A least squares fit of a single Gaussian to each observed line profile gives the peak line intensity, I , the relative line-of-sight velocity, v , and the line width, $w = FWHM/(2\sqrt{\ln 2})$. We estimate the accuracy in the relative line-of-sight velocity determinations to be 1 km s^{-1} for O v $\lambda 629$ and 1.5 km s^{-1} (2 km s^{-1}) for N v $\lambda 1238$ ($\lambda 1242$).

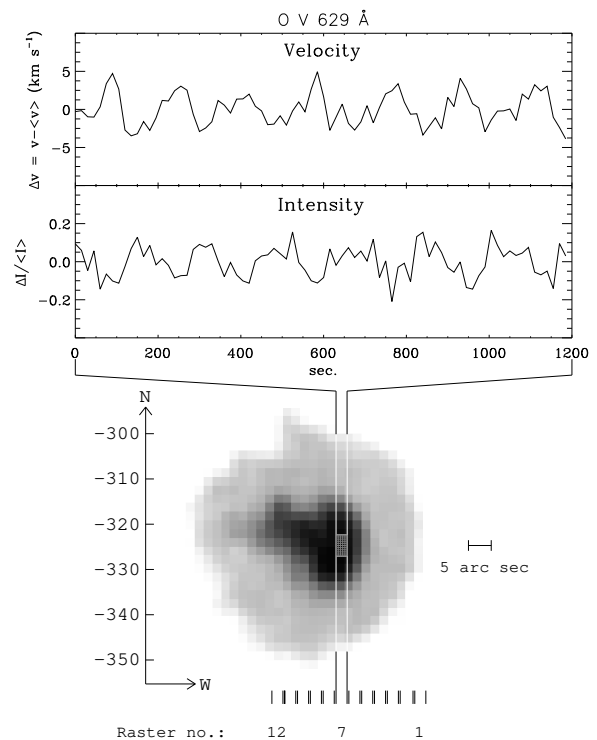


Fig. 1.— Observed O v $\lambda 629$ oscillations in relative line-of-sight velocity, $\Delta v = v - \langle v \rangle$, and relative peak intensity, $\Delta I / \langle I \rangle$, in the center of the umbra, see hatched area in the sunspot image, observed with the MDI instrument (Scherrer et al. 1995).

From the SUMER observations alone it is difficult to separate temporal from spatial changes in oscillatory power. Simultaneous observations with the Coronal Diagnostic Spectrometer (CDS; Harrison et al. 1995) in ten emission lines, including the O v $\lambda 629$ line, with a cadence of 25 min, show only small tempo-

ral variations in the overall intensity and line-of-sight velocity patterns during the time span of the observations. For a description of sunspot velocity field observations with CDS, see Brynildsen et al. (1998). The CDS results encourage us to use the SUMER observations to investigate the spatial distribution of the power in the transition region oscillations. By deriving the observed characteristics within each raster for $2''$ sections along the slit the power distribution is studied within an area of $33.5'' \times 90''$ with a spatial resolution of $2.2'' \times 2''$.

3. Results

As an example Figure 1 shows the observed O v $\lambda 629$ umbral oscillations in relative line-of-sight velocity, $\Delta v = v - \langle v \rangle$, and relative peak line intensity, $\Delta I / \langle I \rangle$. The hatched area in the umbra marks the location of this oscillation. Slow variations in the background fields have been removed from the average values, $\langle v \rangle$ and $\langle I \rangle$. This corresponds to applying a low frequency filter in the Fourier domain. Note that the observed oscillations are linear in character without clear signs of shocks. The amplitudes of the oscillations are listed in Table 1.

Table 1: OSCILLATION AMPLITUDES - SEE FIGURE 1

Line	Velocity (km s^{-1})	Peak Intensity (%)
O v $\lambda 629$	2.7	11
N v $\lambda 1238$	2.4	9
N v $\lambda 1242$	2.7	10

Figure 2 shows the corresponding power spectra for the oscillations in line-of-sight velocity and peak line intensity. The power spectra are nearly identical with one maximum within the frequency interval 5.0 - 6.7 mHz, corresponding to periods between 150 and 200 s, and maximum power close to 170 s. We also find a 5% variation in the line width. The corresponding power spectrum is similar to those shown in Figure 2, but is more noisy. The results are scrutinized by tests where artificial noise is added to the observed signal and new values of the line parameters are derived. The tests show that the results for the intensity and the line-of-sight velocity oscillations are confirmed, but the results are less certain for the line width.

Figure 1 shows near temporal coincidence of maxima in peak line intensity and maxima in blueshift. From the corresponding power spectra we deduce a

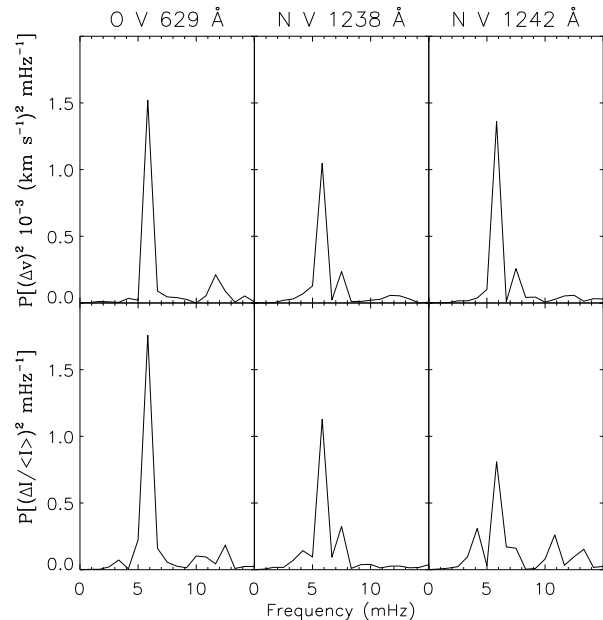


Fig. 2.— Observed power in the transition region sunspot oscillation in line-of-sight velocity and relative peak line intensity for the same position as in Figure 1.

phase difference $\phi_v(629) - \phi_I(629) = 173^\circ$ between the line-of-sight velocity and the peak line intensity for the O v line. The corresponding phase difference for the N v line, $\phi_v(1238) - \phi_I(1238) = 172^\circ$. We give less weight to the observed phase difference of 160° in the $\lambda 1242$ line since this line is weaker than the other lines. In Figure 5, below, we present this phase difference for the O v $\lambda 629$ line for the entire sunspot region.

The determination of the phase difference in velocity or intensity between the N v $\lambda 1238$ and O v $\lambda 629$ lines is difficult since it involves careful alignment along the slit of lines observed in different locations on the detector. For the umbra we find that the wave arrives on average $10 \text{ s} \pm 5 \text{ s}$ earlier in N v $\lambda 1238$ line than in O v $\lambda 629$ line. If the N v line originates at a lower height than the O v line, as seems reasonable considering the temperatures of formation for the N v ($1.5 \times 10^5 \text{ K}$) and O v ($2.1 \times 10^5 \text{ K}$) lines, this suggests an upward propagating wave.

Consider next the observed variation along the slit in raster 7, i.e. in the $2.2'' \times 90''$ wide raster that includes the central part of the umbra. Figure 3 gives the O v $\lambda 629$ variations in peak line intensity, $\Delta I / \langle I \rangle$, and relative line-of-sight velocity,

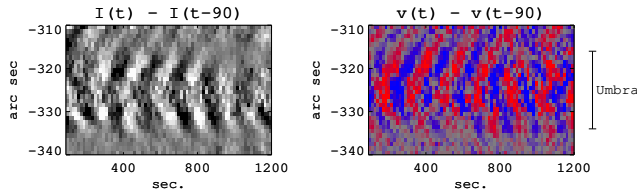


Fig. 3.— Observed O v $\lambda 629$ variation in relative peak line intensity (left) and line-of-sight velocity (right) along the slit in raster 7. Blue (red) color corresponds to motion towards (away from) the observer. To enhance the visibility, the observed signal at time t is subtracted from the observed signal at time $t - 90$ s - this time difference is close to half the wave period, 170 s.

$v - \langle v \rangle$, as a function of time and position along the slit. The visibility and shape of the oscillation wave front is enhanced by subtracting the observed signal at time t from the signal observed at $t - 90$ s, a time difference close to half of the dominant period. Figure 3 shows that waves with periods close to 170 s are observed mainly within the umbra and do not extend into the penumbra to any great extent. The wave front in the central part of the umbra leads the wave front at the rim of the umbra by nearly a full wave period. Clearly the observed oscillation affects the entire umbral transition region, but the generation or transmission of the wave depend on the position within the umbra.

To investigate the suggestion by Gurman et al. (1982) that the oscillations are caused by upward propagating acoustic waves, we make use of the property that the relative perturbation in number density, $\Delta N/N_0$, varies in phase with the line-of-sight velocity, v_{\parallel} , (e.g. Hansteen & Maltby 1992). Regarding v_{\parallel} as positive when directed away from the observer we may write,

$$\frac{v_{\parallel,m}}{v_S} \sin(\omega t - kz) = -\cos\theta \frac{\Delta N_m}{N_0} \sin(\omega t - kz) \quad (1)$$

for an upward propagating acoustic wave with a sinusoidal variation. Here v_S is the sound speed, θ is the aspect angle and the index m denotes the amplitude. For N v and O v, formed in a gas with a mean molecular weight of 0.60 at temperatures close to 1.5×10^5 K and 2.1×10^5 K, we estimate the sound speeds to be 58 km s^{-1} and 69 km s^{-1} . We will use equation

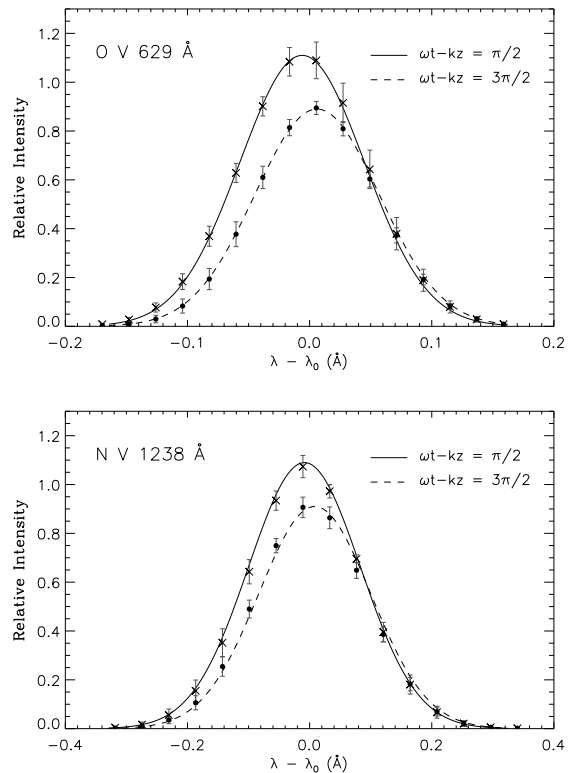


Fig. 4.— Comparison of calculated line profiles that are formed in a region pervaded by upward propagating acoustic waves and observed values (dots and crosses), for $(\omega t - kz) = \pi/2$ and $3\pi/2$. The r.m.s. deviations between six observed values with the same phase are shown. The sunspot is located at $\theta = 40^\circ$.

(1) to calculate line profiles that may be compared with observations. Since the lines may be regarded as optically thin, the intensity is determined by an integration along the line-of-sight of the product of the line profile, the electron number density, N_e , the N v (O v) ion density, N_i , and a temperature dependent function, $g(T_e)$ (e.g. Mariska 1992). The influence of the wave on the function $g(T_e)$ is small (e.g. Gurman et al. 1982). Assuming ionization balance, such that $N_i \propto N_e$, and neglecting possible variations in the thickness of the transition region, we may write the line intensity as $I_\nu(\theta) \propto N_e^2 \propto N^2$. This implies that we may use the observed intensity amplitudes of 9% and 11%, see Table 1, to determine the corresponding density amplitudes and equation (1) to calculate the line profile for different values of $(\omega t - kz)$. Figure 4

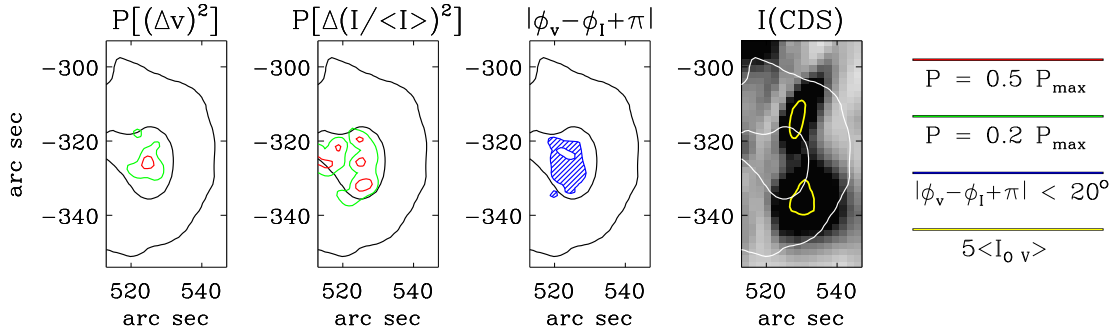


Fig. 5.— Left to right: Spatial distribution of the O v $\lambda 629$ power in relative line-of-sight velocity, relative peak line intensity, phase difference $|\phi_v - \phi_I + \pi|$, and the CDS peak line intensity image, where sunspot plumes with $I \geq 5 \times \langle I \rangle$ are marked with yellow contours. The contours of the umbra and penumbra are shown.

shows the calculated line profiles for O v $\lambda 629$ and N v $\lambda 1238$, with $\Delta N_m/N_0 = 0.055$ and $\Delta N_m/N_0 = 0.045$, and line broadening owing to the instrument and non-thermal velocities of 27 km s^{-1} and 24 km s^{-1} , respectively. For $(\omega t - kz) = \pi/2$ both the peak line intensity and the line shift towards shorter wavelengths reach their maxima, whereas for $(\omega t - kz) = 3\pi/2$ a maximum in line shift towards longer wavelengths occurs while the peak line intensity reaches a minimum.

The observed values at each wavelength are averages of six intensity values from the center of the umbra at the corresponding phases. The averages are determined from the time series in raster 7, where six minima and maxima are observed. The average is constructed from a $2''$ wide strip centered at position $-326''$, see Figure 3. The agreement between observed and calculated profiles in Figure 4 is remarkable and supports the interpretation of the oscillations as caused by upward propagating acoustic waves. To obtain a deeper understanding of this result, the wave propagation through the transition region should be thoroughly discussed, see Zugzda, Staude, & Locans (1984) for a discussion of this topic.

Figure 5 gives the spatial distributions of power in line-of-sight velocity and peak line intensity oscillations between $5.0 - 6.7 \text{ mHz}$ for the O v $\lambda 629$ line. The phase difference $|\phi_v - \phi_I + \pi| < 20^\circ$ throughout most of the umbra, i.e. the maximum intensity is nearly in phase with the maximum velocity directed towards the observer. The oscillations are restricted to the umbra and interestingly, the spatial distributions of power in velocity and intensity differ. Whereas the power in velocity shows one maximum, the power in

intensity also show maxima closer to the umbral rim, not far from the sunspot plumes observed with CDS (Figure 5, right), the plumes have peak line intensity $I \geq 5 \times \langle I \rangle$. For a recent discussion of sunspot plumes, see Brynildsen et al. (1998). Possibly the direction of wave propagation changes with position in the umbra.

In summary, significant oscillations in line-of-sight velocity and peak line intensity are observed, with periods close to 170 s . The observed transition region oscillations are concentrated to the umbra and the entire umbral transition region oscillates. We study the observed line profiles and find support for the suggestion that the waves are upward propagating acoustic waves. Discussions of the relation between the shock waves observed in the chromosphere and the present observations are of interest, but outside the scope of this letter.

We are indebted to the international SUMER team and thankful to the MDI team for permission to use their data. SUMER is supported by DLR, CNES, NASA and the ESA Prodex programme (Swiss contribution). SOHO is a project of international cooperation between ESA and NASA.

REFERENCES

- Bard, S. & Carlsson, M. 1997 in Fifth SOHO Workshop: The Corona and Solar Wind Near Minimum Activity, ed. A. Wilson, ESA SP-404, 189
- Beckers, J. M. & Tallant, P. E. 1969, Sol. Phys., 7, 351

- Brynildsen, N., Maltby, P., Brekke, P., Fredvik, T.,
Haugan, S. V. H., Kjeldseth-Moe, O., & Wikstøl,
Ø. 1998, ApJ, 502, L85
- Giovanelli, R. G. 1972, Sol. Phys. 27, 71
- Gurman, J. B., Leibacher, J. W., Shine, R. A.,
Woodgate, B. E., & Henze, W. 1982, ApJ, 253,
939
- Hansteen, V. & Maltby, P. 1992, Comments on As-
trophys., 16, 137
- Harrison, R. A. et al. 1995, Sol. Phys., 162, 233
- Henze, W., Tandberg-Hanssen, E., Reichmann, E. J.,
& Athay, R. G. 1984, Sol. Phys., 91, 33
- Lites, B. W. 1992 in Sunspots: Theory and Observa-
tions, ed. J. H. Thomas & N. O. Weiss (Dordrecht,
Kluwer), 261
- Mariska, J. T. 1992, The Solar Transition Region
(Cambridge, Cambridge Univ. Press)
- Rendtel, J., Staude, J., Innes, D., Wilhelm, K., &
Gurman, J. B. 1998 in A Crossroads For European
Solar and Heliospheric Physics, ed. R. A. Harris,
ESA SP-417, 277
- Scherrer, P. H. et al. 1995, Sol. Phys., 162, 129
- Thomas, J. H., & Weiss, N. O. 1992 in Sunspots:
Theory and Observations, ed. J. H. Thomas & N.
O. Weiss (Dordrecht, Kluwer), 3
- Wilhelm, K. et al. 1995, Sol. Phys., 162, 189
- Zirin, H. & Stein, A. 1972, ApJ, 178, L85
- Zugzda, Y. D., Staude, J., & Locans, V. 1984, Sol.
Phys., 91, 219